



Universität Stuttgart

**iew**  
Institut für  
Elektrische Energiewandlung

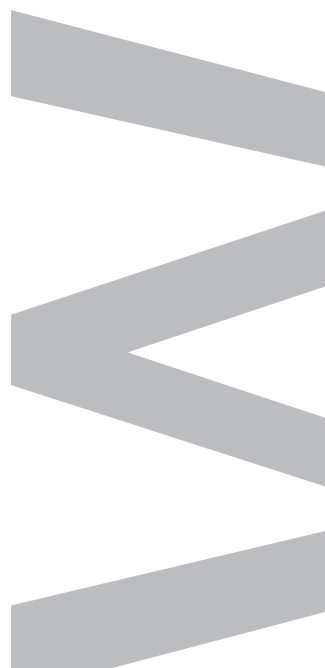
Berichte aus dem Institut für Elektrische Energiewandlung

**Samuel Müller**

Inductive Electrically Excited Synchronous Machines  
for Electrical Vehicles



**Band 14**



**Inductive Electrically Excited Synchronous Machines  
for Electrical Vehicles**

**Von der Fakultät Informatik, Elektrotechnik  
und Informationstechnik der Universität Stuttgart  
zur Erlangung der Würde des Doktor-Ingenieurs (Dr.-Ing.)  
genehmigte Abhandlung**

**Vorgelegt von  
Samuel Wilhelm Müller  
aus Böblingen**

**Hauptberichterin: Prof. Dr.–Ing. Nejila Parspour  
Mitberichter: Prof. Dr.–Ing. Dieter Gerling**

**Tag der mündlichen Prüfung: 07.03.2023**

**Institut für Elektrische Energiewandlung  
der Universität Stuttgart**

**2023**



Berichte aus dem Institut für Elektrische Energiewandlung

Band 14

**Samuel Müller**

**Inductive Electrically Excited Synchronous Machines  
for Electrical Vehicles**

D 93 (Diss. Universität Stuttgart)

Shaker Verlag  
Düren 2023

**Bibliographic information published by the Deutsche Nationalbibliothek**

The Deutsche Nationalbibliothek lists this publication in the Deutsche Nationalbibliografie; detailed bibliographic data are available in the Internet at <http://dnb.d-nb.de>.

Zugl.: Stuttgart, Univ., Diss., 2023

Copyright Shaker Verlag 2023

All rights reserved. No part of this publication may be reproduced, stored in a retrieval system, or transmitted, in any form or by any means, electronic, mechanical, photocopying, recording or otherwise, without the prior permission of the publishers.

Printed in Germany.

ISBN 978-3-8440-9139-7

ISSN 2196-9213

Shaker Verlag GmbH • Am Langen Graben 15a • 52353 Düren

Phone: 0049/2421/99011-0 • Telefax: 0049/2421/99011-9

Internet: [www.shaker.de](http://www.shaker.de) • e-mail: [info@shaker.de](mailto:info@shaker.de)

# Preface

This thesis emerged during my work as research associate at the Institute of Electrical Energy Conversion at the University of Stuttgart. First, I want to express special thanks to my main supervisor Prof. Dr.-Ing. Nejila Parspour, who supported and encouraged me in this work and throughout my work at the Institute.

Further, I would like to thank Prof. Dr.-Ing. Dieter Gerling for co-supervising and the interest in this work.

This project was mainly financed by the Vector Stiftung. I appreciate the support of this work from them, namely Mr. Hinderer, Mr. Litschel and Mr. Schelling. It was essential for the emergence of this work.

A big thank you goes to the workshop, especially to Mr. Hermann Kattner, for supporting the construction of the prototype.

I am very grateful to my colleagues for supporting me in every challenge, the good cooperation and the motivation for this work.

The student theses and research assistants were necessary for the outcome of this thesis. Special thanks go to Julius Weber, Marco Arndt, Christine Futterlieb, Zhimin Li and Fabian Gieck.

Finally, a big thank you goes to my wife Maria, who motivated and supported me to finish this work.

Stuttgart, June 2023

Samuel Wilhelm Müller



# Abstract

Due to the strong growth of electromobility, the demand for compact and efficient electric motors is increasing. Currently, mainly permanent magnet synchronous machines are used for electric vehicles. The use of rare earth materials in the magnets is cost-sensitive and decreases the efficiency in the field-weakening range at high speeds. An alternative is the use of electrically excited synchronous machines. Electrically excited synchronous machines are often used as generators. For this purpose, power density, wear and operation over the entire operating range are not relevant but are essential for use in electric vehicles.

This doctoral thesis presents an inductive electrically excited synchronous machine with a contactless energy transmission system. The transmission system is integrated inside the rotor shaft to reduce axial length. The model of an electrically excited synchronous machine is extended by considering saturation. An analytical calculation for the transformation ratio is derived. Furthermore, rotor shape is investigated for operation in field weakening.

During the design process, thermal and mechanical requirements are considered in addition to an electromagnetic design, and the topology selection of the contactless energy transmission system is explained. An electromagnetic optimization method is developed and applied to minimize torque ripple and optimize efficiency in the drive cycle. For this purpose, a vehicle model is used to derive a relevant operating range from the driving cycle. In simulation, the machine losses in the driving cycle are reduced by 40 % compared to referenced permanent magnet excited synchronous machine.

The optimized machine is built as a prototype with an integrated contactless energy transmission system, driven on the test bench and evaluated.





# Zusammenfassung

Durch den starken Zuwachs der Elektromobilität steigt der Bedarf an kompakten und effizienten Elektromotoren. Aktuell werden für Elektrofahrzeuge hauptsächlich permanentmagnetisch erregte Synchronmaschinen eingesetzt. Der Einsatz von seltenen Erden in den Magneten ist sowohl kostensensitiv als auch nachteilig für den Wirkungsgrad im Feldschwähebereich bei hohen Drehzahlen. Eine Alternative ist der Einsatz von elektrisch erregten Synchronmaschinen.

Elektrisch erregte Synchronmaschinen werden häufig als Generatoren eingesetzt. Für diesen Zweck sind Leistungsdichte, Verschleiß und Betrieb im gesamten Betriebsbereich nicht relevant, für den Einsatz in Elektrofahrzeugen jedoch essenziell.

In dieser Doktorarbeit wird eine induktiv elektrisch erregte Synchronmaschine mit kontaktlosem Energieübertragungssystem vorgestellt. Zur Reduktion der axialen Länge ist das Übertragungssystem in den Rotor integriert. Es wird dafür die Modellierung der elektrisch erregten Synchronmaschine um die Berücksichtigung der Sättigung ergänzt und eine analytische Berechnung des, für die Modellierung notwendigen, Übersetzungsverhältnisses hergeleitet. Desweiteren wird das Rotordesign für Betrieb in Feldschwäche untersucht.

Beim Design des Systems werden dabei neben einer elektromagnetischen Auslegung auch thermische und mechanische Anforderungen berücksichtigt sowie eine Topologieauswahl des Übertragungssystems erläutert. Eine elektromagnetische Optimierung wird entwickelt und zur Minimierung der Drehmomentwelligkeit und Optimierung des Wirkungsgrades im Fahrzyklus angewandt. Dazu wird mit Hilfe eines Fahrzeugmodells aus dem Fahrzyklus ein relevanter Betriebsbereich abgeleitet.

Die optimierte Maschine wird mit integriertem Übertragungssystem als Prototyp aufgebaut, am Prüfstand in Betrieb genommen und ausgewertet.



# Table of Contents

List of Tables	XIII
List of Figures	XV
List of Abbreviations	XIX
List of Symbols	XXIII
<b>1 Introduction</b>	<b>1</b>
<b>2 Requirements and Driving Cycle Analysis</b>	<b>3</b>
2.1 Literature review . . . . .	4
2.2 BMW i3 . . . . .	6
2.2.1 Electrical drive train . . . . .	8
2.2.2 Vehicle model . . . . .	10
2.3 Driving cycle . . . . .	14
2.4 Model for driving cycle analysis . . . . .	15
2.4.1 Driver . . . . .	15
2.4.2 Control unit . . . . .	17
2.4.3 Electrical drive . . . . .	17
2.4.4 Battery . . . . .	17
2.5 Simulation . . . . .	18
2.5.1 Model verification . . . . .	18
2.5.2 Operation points of the electrical machine . . . . .	19
2.5.3 Selection of the important operating points for the optimization . . . . .	21
2.6 Requirements for the iEESM . . . . .	22

<b>3</b>	<b>Model and Operation Strategies of EESMs</b>	<b>23</b>
3.1	Air-gap Transformer . . . . .	24
3.1.1	Linear Magnetization . . . . .	24
3.1.2	Nonlinear Magnetization . . . . .	26
3.2	Fundamental-wave model of an EESM . . . . .	29
3.3	Transformation Ratio $a_{\text{eff}}$ in EESMs . . . . .	32
3.3.1	Stator Winding Factor . . . . .	32
3.3.2	Rotor Winding Factor . . . . .	33
3.3.3	Comparison of Rotor Winding Factors for different Rotor Shapes . . . . .	40
3.4	Losses in Electrically Excited Synchronous Machines . . . . .	42
3.4.1	Mechanical Losses . . . . .	43
3.4.2	Copper Losses . . . . .	43
3.4.3	Iron Losses . . . . .	44
3.4.4	Energy Transmission System . . . . .	45
3.5	Operation Strategies . . . . .	46
3.5.1	Maximum Torque per Ampere . . . . .	46
3.5.2	Maximum Efficiency . . . . .	47
3.5.3	Rotor Shape for Field Weakening . . . . .	47
<b>4</b>	<b>Design and Construction</b>	<b>51</b>
4.1	Challenges of Designing an iEESM . . . . .	51
4.2	Electromagnetic Design . . . . .	53
4.2.1	Analytical-empirical Design . . . . .	54
4.2.2	Winding Definition and Determination of the Number of Pole Pairs . . . . .	54
4.2.3	FEA-Modeling . . . . .	56
4.3	Thermal Design . . . . .	57
4.3.1	Maximum Continuous Power . . . . .	59
4.3.2	Thermal Overload Capability . . . . .	62
4.4	Rotary Contactless Energy Transmission System . . . . .	65
4.5	Mechanical Design . . . . .	67
4.6	Construction . . . . .	71
4.6.1	Motor parts . . . . .	71
4.6.2	Placement of the CET-System . . . . .	72
4.6.3	Overall Construction . . . . .	74

<b>5</b>	<b>Operation Point-Dependent Optimization</b>	<b>75</b>
5.1	Overview and Literature Review . . . . .	76
5.1.1	Obtaining the Solution Space . . . . .	78
5.1.2	Overview of the optimization algorithms . . . . .	79
5.1.3	Selected optimization algorithms . . . . .	80
5.2	Optimization Routine . . . . .	82
5.3	FEA-Model . . . . .	83
5.3.1	Parameterized Geometry . . . . .	83
5.3.2	Multi-Static Model . . . . .	85
5.3.3	Losses . . . . .	88
5.4	Cost calculation . . . . .	88
5.4.1	Winding optimization . . . . .	89
5.4.2	Solve . . . . .	91
5.4.3	MTPA with maximum current . . . . .	92
5.4.4	Termination criterion 1 . . . . .	92
5.4.5	Calculate corner point and fix point factor . . . . .	92
5.4.6	MTPA for operating point . . . . .	94
5.4.7	Termination criterion 2 . . . . .	94
5.4.8	Determine weighted costs for $\eta$ and $T_{\text{shaft}}$ . . . . .	95
5.5	Geometry optimization . . . . .	95
5.5.1	Reducing the degrees of freedom . . . . .	96
5.5.2	Final Optimization Results and Design Selection . . . . .	99
5.5.3	Simulated Driving Cycle Results . . . . .	101
5.6	Conclusion and Further Optimization Possibilities . . . . .	102
<b>6</b>	<b>Control and Measurement on the test bench</b>	<b>103</b>
6.1	Control System . . . . .	104
6.2	Prototype and test bench setup . . . . .	106
6.3	Parameter identification . . . . .	109
6.3.1	Stator Short Circuit Measurement . . . . .	109
6.3.2	Flux Linkage and Inductance Maps . . . . .	109
6.3.3	Saliency ratio . . . . .	112
6.4	Efficiency Map . . . . .	113
6.5	Temperature Measurement . . . . .	115
<b>7</b>	<b>Conclusion and Outlook</b>	<b>117</b>
	<b>Bibliography</b>	<b>121</b>

## Table of Contents

---

<b>A</b>	<b>Requirements on the iEESM</b>	<b>135</b>
<b>B</b>	<b>BMW i3 Data</b>	<b>137</b>
<b>C</b>	<b>Rotor Shape</b>	<b>141</b>
C.1	Determination of Air-gap Length for EESMs with Rotor Tooth Radius . . . . .	141
C.2	Rotor Geometry for Sinusoidal Flux Distribution . . . . .	144
<b>D</b>	<b>Used Software</b>	<b>145</b>
<b>E</b>	<b>Optimization Algorithms</b>	<b>147</b>
E.1	Genetic Algorithm . . . . .	147
E.2	Global Optimization Toolbox in MATLAB . . . . .	150
E.2.1	The GlobalSearch solver . . . . .	151

# List of Tables

2.1	Overview of literature for driving cycle analyses . . . . .	5
2.2	BMW i3 (94 Ah) battery and inverter data, and derived requirements for the iEESM . . . . .	8
2.3	BMW i3 electrical machine data and derived requirements for the iEESM . . . . .	11
2.4	Driver and control unit parameter . . . . .	16
2.5	Simulated energy consumption of the i3 in the WLTC drive cycle . . . . .	18
3.1	Rotor winding factors for non zero harmonics depending on rotor geometry . . . . .	42
4.1	Winding definition . . . . .	56
4.2	Determined parameter space based on nonlinear 2D-FEA . . . . .	57
4.3	Basic data of the chosen water jacket . . . . .	57
4.4	Thermal analysis of the final geometry at rated point for continuous and continuous periodic (S6) . . . . .	61
4.5	Requirements and boundary conditions of the CET-System for the electromagnetic design . . . . .	67
4.6	Requirements of the design for mechanical strength . . . . .	67
5.1	Geometry parameters . . . . .	86
5.2	Settings and boundary conditions of the optimization routine . . . . .	96
5.3	Relation of yoke height to tooth width for initial analysis and final optimized machine. . . . .	98
5.4	Analysis of number of poles and rotor diameter. The obtained range and the chosen value for final optimization is listed. . . . .	98
5.5	Simulation results of the finally chosen geometry . . . . .	100



5.6	Energy consumption WLTC driving cycle simulation results for the i3. The losses are sorted descending. . . . .	102
A.1	Requirements on the iEESM for design and optimization . . . . .	136
B.1	BMW i3 battery and inverter data . . . . .	137
B.2	BMW i3 Vehicle data . . . . .	138
B.3	BMW i3 electrical machine data . . . . .	139
D.1	Software versions used in this work . . . . .	145
E.1	solver choice in Global Optimization Toolbox . . . . .	150

# List of Figures

2.1	BMW i3 of the IEW extended with inductive charging . . . .	7
2.2	BMW i3 electrical machine . . . . .	9
2.3	Measured BMW i3 machine efficiency map . . . . .	10
2.4	Overview vehicle model . . . . .	10
2.5	Forces on the longitudinal vehicle model on a inclined plane	12
2.6	Speed dependend power consumption of the BMW i3 (slope 4 %) . . . . .	14
2.7	Driving Cycle WLTC Class 3 . . . . .	14
2.8	Driving cycle analysis model . . . . .	16
2.9	Machine operating points determined by driving cycle analysis	20
2.10	Energy consumption for the i3 during WLTC Class 3 . . . . .	22
3.1	2D model of the air-gap transformer . . . . .	24
3.2	Equivalent electrical circuit of an air-gap transformer with linear magnetic materials . . . . .	26
3.3	Equivalent electrical circuit for an air-gap transformer with non- linear materials . . . . .	27
3.4	Simulation results of the transformer compared with the model- ing using the T-EC . . . . .	28
3.5	Reference systems for field oriented controlled EESM . . . . .	30
3.6	Dynamic equivalent electrical circuit in dq-frame for EESMs	31
3.7	Geometry and air-gap flux of a salient-pole rotor considering pole covering factor $a_{pol} < 1$ . . . . .	35
3.8	Geometry of a salient-pole rotor considering pole covering factor $a_{pol} < 1$ and a rounded shaped tooth . . . . .	37
3.9	Geometry and air-gap flux of a salient-pole rotor considering pole covering factor $a_{pol} < 1$ and a rounded shaped tooth . . . . .	38

3.10	True to scale geometry of rotor shape for the prototype compared to rotor shape for ideal sinusoidal air-gap flux density . . . . .	39
3.11	Air-gap flux density for different rotor shapes . . . . .	40
3.12	Influence of $a_{\text{pol}}$ on winding factors for rotor shapes with rectangular, tooth radius and drop shape for fundamental frequency, 5 <sup>th</sup> and 7 <sup>th</sup> harmonic . . . . .	41
3.13	Frequency spectrum of rotor winding factor . . . . .	42
3.14	Influence of excitation current on saturation and impact on saliency. . . . .	49
3.15	Inductances and torque determined with frozen permeability method . . . . .	50
4.1	Overview of the multi-physics design challenge of an iEESM	52
4.2	Frequency spectrum of the three-phase $\mathcal{F}$ for integer-slot winding with $p = 4$ . . . . .	55
4.3	Design of the cooling system for the EESM . . . . .	58
4.4	Thermal simulation results of the optimized machine . . . . .	60
4.5	Steady state power loss Sankey-Diagram at rated power . . . . .	63
4.6	Transient thermal simulation at overload operation . . . . .	64
4.7	Transient thermal simulation in continuous periodic operation	65
4.8	Possibilities for the setup of the coil system . . . . .	66
4.9	Mechanical simulation of a single tooth of the final geometry at maximum speed (105 Nm@11400 rpm) . . . . .	69
4.10	Components to increase the strength of the rotor . . . . .	70
4.11	Construction of the rotor . . . . .	71
4.12	Construction of the stator . . . . .	72
4.13	Possibilities for the placement of the CET-System . . . . .	73
4.14	Construction of the complete system iEESM . . . . .	74
5.1	Structure of optimization processes . . . . .	77
5.2	Overview of the optimization routine . . . . .	83
5.3	Geometry parameters shown on the drawing of the final geometry . . . . .	84
5.4	Torque ripple over electrical angle for 360, 30 and 11 points per cycle . . . . .	87
5.5	Flow chart of the cost calculation . . . . .	90
5.6	Geometry parameters of rotor winding . . . . .	91

5.7	Qualitative characteristic of torque and power over speed with required torque and power . . . . .	93
5.8	Qualitative characteristic for the fix point factor depended on the constraints in the corner point . . . . .	94
5.9	Flux density at operation point 40 Nm@9000 rpm . . . . .	97
5.10	Optimization result for variable $D_{R,o}$ . . . . .	98
5.11	Pareto diagram for final optimization . . . . .	99
5.12	Efficiency map of the finally chosen geometry . . . . .	101
6.1	Overview of the control system . . . . .	105
6.2	Setup of the rotor of the prototype . . . . .	107
6.3	Prototype iEESM and test bench setup . . . . .	108
6.4	Stator short circuit measurement for excitation current up to $i_c = 10$ A . . . . .	109
6.5	Measured flux linkages $\lambda_d$ and $\lambda_q$ . . . . .	110
6.6	Absolute inductances derived from flux linkage measurement . . . . .	111
6.7	Saliency ratio $L_{q,abs}/L_{d,abs}$ for constant excitation current $i_c$ . . . . .	113
6.8	Measured efficiency of the iEESM, compared with measured efficiency of the reference PMSM and simulated iEESM efficiency . . . . .	114
6.9	Measurement of rotor temperature for continuous operation . . . . .	115
6.10	Measurement of rotor temperature for periodic operation . . . . .	116
A.1	Requirements on torque-speed characteristic for the iEESM in motor mode . . . . .	135
C.1	Geometry of a salient-pole rotor considering pole covering factor $a_{Pol} < 1$ and a rounded shaped tooth . . . . .	142
C.2	Triangle with notations . . . . .	143
C.3	Optimal rotor pole geometry for ideal sinusoidal air-gap flux density . . . . .	144
E.1	Flowchart Genetic algorithm . . . . .	149
E.2	representation of the object function of the example . . . . .	151
E.3	workflow of the optimization algorithm GlobalSearch . . . . .	152



# List of Abbreviations

<b>Notation</b>	<b>Description</b>
AC	Alternating current
ADAC	Allgemeiner Deutsche Automobil-Club e. V.
ARTEMIS	Assessment and Reliability of Transport Emission Models and Inventory Systems
AWG	American Wire Gauge
BMW	Bayrische Motorenwerke AG
CAD	Computer-aided design
CET	Contactless energy transfer
D.E.	Drive End
DC	Direct current
DOE	Design of experiments
EC	Equivalent circuit
EESM	Electrically Excited Synchronous Machine
EM	Electrical Machine
EU	European Union
EV	Electrical Vehicle
FE	Finite element
FEA	Finite element analysis
FOC	Field oriented control
FPGA	Field-programmable gate array

## List of Abbreviations

---

<b>Notation</b>	<b>Description</b>
GA	Genetic algorithm
GFRP	Glass-Fibre Reinforced Plastic
HIL	Hardware-in-the-loop
HWFET	Highway Fuel Economy Driving Schedule
iEESM	Inductive Electrically Excited Synchronous Machine
IEW	Institute of Electrical Energy Conversion
IGBT	Insulated-Gate Bipolar Transistor
IR	Infrared
LHS	Latin hypercube sampling
LUT	Lookup table
MATLAB	Software „matrix laboratory“ from MathWorks®
MDE	Maximum drive efficiency
ME	Maximum efficiency
MTPA	Maximum torque per ampere
N.D.E.	Non-Drive End
NEDC	New European Driving Cycle
NSGA	Non-dominated sorting genetic algorithm
PLL	Phase-locked loop
PM	Permanent Magnet
PMASR	Permanent Magnet Assisted Synchronous Reluctance Motor
PMSM	Permanent Magnet Synchronous Machine
PWM	Pulse-width modulation
SMC	Soft magnetic composite
SVPWM	Space Vector Pulse Width Modulation
TFM	Transverse Flux Machine
UDDS	Urban Dynamometer Driving Schedule
USo6	US driving cycle number 06

<b>Notation</b>	<b>Description</b>
VW	Volkswagen
WLTC	Worldwide harmonized Light vehicles Test Cycle
WLTP	Worldwide harmonized Light vehicles Test Procedure





# List of Symbols

Symbol	Unit	Description
$a_{\text{eff}}$	—	Effective transformation ratio
$A_f$	$\text{m}^2$	Vehicle frontal area
$a_{\text{coils,par}}$	—	Number of parallel coils on stator
$a_{\text{Pol}}$	—	Pole coverage factor (ratio of rotor tooth width related to $\tau_p$ )
$a_{\text{Saliency}}$	—	Saliency ratio
$a_{\text{coils,ser}}$	—	Number of serial coils on stator
$a_{\text{coils,serR}}$	—	Number of serial coils on rotor
$a_{\text{turn}}$	—	Turns ratio
$A_{\text{wire}}$	$\text{mm}^2$	Wire diameter
$B$	T	Absolute of magnetic flux density
$B_\delta$	T	Absolute of air-gap magnetic flux density
$\hat{B}_\delta$	T	Maximum of air-gap magnetic flux density
$\hat{B}$	T	Maximum of magnetic flux density
$b_s$	mm	Slot opening
$C_{\text{Batt,eff}}$	kWh	Effective battery capacity
$C_{\text{Batt,n}}$	Ah	Nominal battery capacity
$C_{\text{circ}}$	m	Circumference of a circle
$c_D$	—	Drag coefficient
$C_{\text{esson}}$	$\text{VA}^{\text{min}}/\text{m}^3$	Esson's utilization factor
$c_{\text{Fe,exc}}$	W	Iron loss coefficient for excess losses

## List of Symbols

---

Symbol	Unit	Description
$c_{\text{Fe,eddy}}$	—	Iron loss coefficient for eddy current losses
$c_{\text{Fe,hyst}}$	—	Iron loss coefficient for hysteresis losses
$c_{\text{R}}$	—	Rolling friction coefficient
$c_{\text{windage}}$	$\text{Nm}/\text{s}^2$	Windage loss coefficient
$D_{\text{R,Polesurface}}$	mm	Rotor pole surface diameter
$D_{\text{R,o}}$	mm	Rotor outer diameter
$D_{\text{S,in}}$	m	Stator inner diameter
$D_{\text{S,out}}$	m	Stator outer diameter
$D_{\text{Shaft}}$	mm	Shaft diameter
$D_{\text{S,o}}$	mm	Stator outer diameter
$D_{\text{S,i}}$	mm	Stator inner diameter (stator bore diameter)
$e$	—	Euler's number
$f$	$1/\text{s}$	Electrical frequency
$F_0$	$\text{mm}^{\text{P}}$	Auxiliary variable for determination of rotor tooth shape for sinusoidal air-gap flux
$\vec{F}_a$	N	Applied force
$F_{\text{Brake}}$	N	Braking force
$f_{\text{cost,1}}$	—	First cost value
$f_{\text{cost,2}}$	—	Second cost value
$F_{\text{D}}$	N	Drag force
$f_{\text{fund,max}}$	Hz	Maximum fundamental frequency
$\vec{F}_n$	N	Normal force
$F_{\text{R}}$	N	Rolling friction force
$f_{\text{sw}}$	Hz	Swichting frequency
$F_{\text{Traction,EM}}$	N	Traction force due to the electrical machine
$\vec{F}_w$	N	Weight force
$\vec{F}_{w,\text{slope}}$	N	Downhill-slope force
$g$	—	Gear module
$H$	$\text{A}/\text{m}$	Absolute of magnetic field

Symbol	Unit	Description
$\hat{H}_\delta$	A/m	Maximum of air-gap magnetic field
$b_{\text{Poleoffset}}$	mm	Offset of the pole circle center to rotor circle center
$b_{\text{R,coil}}$	mm	Rotor coil height
$b_{\text{R,lam}}$	mm	Rotor lamination height
$b_{\text{R,tip}}$	mm	Rotor tooth tip height
$b_{\text{R,coil}}$	mm	Rotor tooth height
$b_{\text{R,yoke}}$	mm	Rotor yoke height
$b_{\text{S,coil}}$	mm	Stator coil height
$b_{\text{S,lam}}$	mm	Stator lamination height
$b_{\text{S,tip}}$	mm	Stator tooth tip height
$b_{\text{S,yoke}}$	mm	Stator yoke height
$b_{\text{yoke}}$	mm	Yoke height
$i$	A	Current electrical current
$i_1$	A	Primary side current
$i_2$	A	Secondary side current
$i_2'$	A	Secondary side current referred to the primary side
$i_{\text{abc}}$	A	Three phase current
$\underline{i}$	A	Complex current
$i_d$	A	Stator d-axis current in rotor flux reference frame
$i_{\text{dq,meas}}$	A	Measured complex current in d/q frame
$i_{\text{dq,err}}$	A	Complex current deviation in d/q frame
$i_{\text{dq,SP}}$	A	Stator complex setpoint current in d/q frame
$i_{\text{d,SP}}$	A	Stator d-axis setpoint current in rotor flux reference frame
$i_e$	A	Rotor excitation current
$i_e'$	A	Referred rotor excitation current
$I_e$	A	Effective rotor excitation current
$i_{e,\text{max}}$	A	Maximum rotor excitation current
$I_{e,\text{max,lim}}$	A	Limit of the maximum rotor excitation current

## List of Symbols

---

Symbol	Unit	Description
$i_{e,SP}$	A	Rotor excitation setpoint current
$i_{\mu}$	A	Magnetization current in d-axis rotor flux reference frame
$\hat{i}$	A	Current peak value
$I_{\text{phase,max}}$	A	Maximum effective phase current
$i_q$	A	Stator q-axis current in rotor flux reference frame
$i_{q,SP}$	A	Stator q-axis setpoint current in rotor flux reference frame
$I_{S,\text{eff}}$	A	Effective stator phase current
$I_S$	A	Stator current
$\underline{i}_S^{\text{dq}}$	A	Complex stator current in rotor flux reference frame
$I_{S,\text{eff,max}}$	A	Maximum stator current
$j$	—	Imaginary unit
$k$	—	Ordinal number of harmonics
$K_d$	—	Distribution factor
$k_{FP}$	—	Fix point factor in fitness calculation
$k_{FP,\text{Power}}$	—	Fix point factor for power at the corner point
$k_{FP,\text{Torque}}$	—	Fix point factor for torque at the corner point
$K_p$	—	Pitch factor
$k_{\sigma d}$	—	d-axis flux leakage factor
$K_{so}$	—	Slot opening factor
$K_{w,R,\nu}$	—	Harmonics rotor winding factor
$K_{w,R}$	—	Fundamental rotor winding factor
$K_{w,S}$	—	Fundamental stator winding factor
$k_{\text{yoke,tooth}}$	—	Additional yoke to tooth lamination
$L_1$	H	Primary side inductance
$L_{12}$	H	Mutual inductance primary side to secondary side
$L_{1m}$	H	Primary side main inductance
$L_{1\sigma}$	H	Primary side leakage inductance

<b>Symbol</b>	<b>Unit</b>	<b>Description</b>
$L_2$	H	Secondary side inductance
$L_{21}$	H	Mutual inductance secondary side to primary side
$L_{2m}$	H	Secondary side main inductance
$L_{2m}'$	H	Secondary side main inductance referred to the primary side
$L_{2\sigma}$	H	Secondary side leakage inductance
$L_{2\sigma}'$	H	Secondary side leakage inductance referred to the primary side
$l_{act}$	m	Axial length of the active parts
$L_d$	H	Direct inductance
$L_{d,abs}$	H	Absolute d-axis inductance
$L_{d,abs,const.exc.}$	H	Absolute d-axis inductance with constant excitation
$L_{d,diff}$	H	Differential d-axis inductance
$L_{de}$	H	D-axis and excitation axis mutual inductance
$L_{dq,diff}$	H	Differential coupling inductance from q- and d-axis
$L_{e,diff}$	H	Differential excitation inductance
$L'_{e,diff}$	H	Referred differential excitation inductance
$l_{lam}$	mm	Lamination length (axial)
$L_m$	H	Magnetization inductance
$L_{md,abs}$	H	D-axis magnetization inductance
$L_{md,diff}$	H	Differential d-axis magnetization inductance
$L_q$	H	Quadrature inductance
$L_{q,abs}$	H	Absolute q-axis inductance
$L_{qd,diff}$	H	Differential coupling inductance from d- to q-axis
$L_{q,diff}$	H	Differential q-axis inductance
$L_{\sigma d}$	H	D-axis leakage inductance
$L_{\sigma d,diff}$	H	Differential d-axis leakage inductance
$m_{act}$	kg	Mass of the active parts
$m_{tot}$	kg	Total mass

## List of Symbols

---

Symbol	Unit	Description
$m_{\text{vehicle}}$	kg	Vehicle mass
$m$	–	Number of phases
$\mathcal{F}$	A	Magneto-motive force
$\mathcal{F}_{\text{rotor}}$	A	Magneto-motive force on the rotor
$n$	$1/\text{min}$	Speed
$N$	–	Number of turns
$N_1$	–	Primary side number of turns
$N_2$	–	Secondary side number of turns
$N_C$	–	Turns per coil
$n_{\text{CP}}$	rpm	Machine speed at corner point
$n_{\text{CP,max}}$	rpm	Maximum speed possible with the calculated corner point
$n_{\text{meas}}$	rpm	Measured speed of the electrical machine
$n_{\text{EM}}$	rpm	Speed of the electrical machine
$n_{\text{it,CP}}$	–	Maximum iterations for MTPA optimization for the corner point
$n_{\text{it,OP}}$	–	Maximum iterations for MTPA optimization for the operation point
$n_{\text{max}}$	rpm	Maximum speed
$n_{\text{mech}}$	$1/\text{min}$	Mechanical speed
$n_{\text{OP}}$	rpm	Machine speed in operating point
$N_{\text{par}}$	–	Number of parallel strands
$N_{\text{R,coil}}$	–	Turns per coil on rotor
$N_{\text{E}}$	–	Number of excitation turns
$N_{\text{S,coil}}$	–	Turns per coil on stator
$n_{\text{wheel}}$	rpm	Speed of the wheel
$P$	W	Effective active electrical power
$p$	–	Number of pole pairs
$P_{\text{Cu,DC}}$	W	DC copper loss

Symbol	Unit	Description
$P_{Cu,AC}$	W	AC copper loss
$P_{Cu,DC,R}$	W	Rotor DC copper loss
$P_{Cu,DC,S}$	W	Stator DC copper loss
$P_{e,max}$	W	Maximum rotor excitation power
$P_{Fe}$	W	Iron loss
$p_{Fe}$	W/m <sup>3</sup>	Specific iron loss
$P_{Cu,S}$	W	Rotor iron loss
$P_{Fe,S}$	W	Stator iron loss
$P_{fric}$	W	Friction losses
$P_{loss,CET}$	W	Losses in the contactless energy transmission system
$p_{max}$	–	Maximum number of pole pairs
$P_{gen,max}$	W	Maximum mechanical power in generator mode
$P_{mot,max}$	W	Maximum mechanical power
$P_{mot,n}$	W	Nominal mechanical power
$P_{ref,CP}$	W	Reference Power at corner point
$P_{windage}$	W	Windage losses
$q$	–	Slots per pole per phase
$q_R$	–	Number of rotor slots per pole
$Q_S$	–	Number of stator slots
$q_s$	–	Number of stator slots per pole
$\dot{V}_{vent}$	m <sup>3</sup> /min	Ventilation flow rate
$R$	Ω	Electrical resistance
$R_1$	Ω	Primary side resistance
$R_2$	Ω	Secondary side resistance
$R_2'$	Ω	Secondary side resistance referred to the primary side
$r_{dyn}$	cm	Dynamic wheel radius
$R_e$	MPa	Yield strength
$R_G$	–	Gear ratio
$\mathcal{R}$	1/H	Magnetic reluctance



## List of Symbols

---

Symbol	Unit	Description
$R_m$	MPa	Tensile strength
$\mathcal{R}_{Fe,1}$	$1/H$	Magnetic reluctance of the iron on the primary side
$\mathcal{R}_{Fe,2}$	$1/H$	Magnetic reluctance of the iron on the secondary side
$\mathcal{R}_{\delta\sigma,1}$	$1/H$	Magnetic reluctance of the airgap in the primary side leakage path
$\mathcal{R}_{\delta\sigma,2}$	$1/H$	Magnetic reluctance of the airgap in the secondary side leakage path
$\mathcal{R}_{\delta}$	$1/H$	Magnetic reluctance of the airgap
$\mathcal{R}_m$	$1/H$	Main magnetic reluctance
$\mathcal{R}_{\sigma 1}$	$1/H$	Primary side leakage magnetic reluctance
$\mathcal{R}_{\sigma 2}$	$1/H$	Secondary side leakage magnetic reluctance
$R_e$	$\Omega$	Rotor resistance
$R'_e$	$\Omega$	Referred rotor resistance
$R_S$	$\Omega$	Stator phase resistance
$r_{S,Slotcorner}$	mm	Stator slot corner radius
$S\%$	%	Percentage slope
$T$	Nm	Torque
$t$	s	Time
$T_{CP}$	Nm	Torque at corner point
$T_{EM}$	Nm	Machine
$T_{fric}$	Nm	Friction torque
$T_{it,dev\%}$	%	Percental deviation in torque to previous simulation for termination criterion
$T_{mag}$	Nm	Magnetic torque
$T_{max}$	Nm	Maximum torque
$T_{ref}$	Nm	Reference torque
$T_{ref,CP}$	Nm	Reference torque at corner point
$T_{shaft}$	Nm	Mechanical shaft torque
$T_{shaft\sim}$	Nm	Mechanical shaft torque ripple

Symbol	Unit	Description
$T_{\text{wheel}}$	Nm	Wheel torque
$TRV$	$\text{kNm}/\text{m}^3$	Torque per rotor volume
$u_{\text{Limit},v}$	—	Boolean indicates voltage limit reached
$v$	$\text{m}/\text{s}$	Speed
$v_1$	V	Primary side voltage
$v_2$	V	Secondary side voltage
$v_2'$	V	Secondary side voltage referred to the primary side
$v_a$	V	Stator voltage phase a
$v_{\text{abc,SP}}$	V	Three phase setpoint voltage
$V_{\text{act}}$	$\text{m}^3$	Volume of the active elements
$v_b$	V	Stator voltage phase b
$V_{\text{Batt,n}}$	V	Nominal battery voltage
$v_c$	V	Stator voltage phase c
$v_{\text{circ}}$	$\text{m}/\text{s}$	Circumferential speed
$v_{\text{circ,max}}$	$\text{m}/\text{s}$	Maximum circumferential speed
$v_d$	V	Stator d-axis voltage in rotor flux reference frame
$v_{\text{DC}}$	V	DC voltage
$v_{\text{dq,ind}}$	V	Complex induced voltage in d/q frame
$v_{\text{dq,SP}}$	V	Complex setpoint voltage in d/q frame
$v_e$	V	Rotor excitation voltage
$v_e'$	V	Referred rotor excitation voltage
$V_{\text{phase,max}}$	V	Maximum effective phase voltage
$v_q$	V	Stator q-axis voltage in rotor flux reference frame
$V_{\text{rotor}}$	$\text{m}^3$	Rotor volume
$v_{\text{vehicle}}$	$\text{km}/\text{h}$	Vehicle speed
$\dot{V}_{\text{fl}}$	$1/\text{min}$	Fluid flow rate
$w_{\text{tooth}}$	mm	Tooth width
$w_{\text{R,coil}}$	mm	Rotor coil width
$w_{\text{R,tooth}}$	mm	Rotor tooth width

## List of Symbols

---

Symbol	Unit	Description
$w_{R,tip}$	mm	Rotor tooth tip width
$w_{S,Slot}$	mm	Stator slot open
$w_{S,tooth}$	mm	Stator tooth width
$x_{pos}$	mm	X position in 2D plane
$y_{pos}$	mm	Y position in 2D plane
$\alpha_{Skew}$	deg	Rotor skewing angle
$\alpha_{Slope}$	deg	Slope angle
$\alpha_{S,tooth}$	deg	Stator tooth angle
$\beta_{FR}$	rad	Electrical angle of the rotor flux oriented coordinate system
$\beta_{el}$	deg	Current angle in d/q
$\beta_{el,initial}$	deg	Initial current angle in d/q for the optimization process
$\delta$	m	Magnetic air-gap length
$\delta_{CP,Power}$	W	Allowed deviation from corner point power with derating the fitness values
$\delta_{CP,Torque}$	Nm	Allowed deviation from corner point torque with derating the fitness values
$\varepsilon_{el}$	deg	Electrical angle
$\varepsilon_{el,k}$	deg	Electrical angle at discrete time step k
$\varepsilon_{el,k+1}$	deg	Electrical angle at next discrete time step after step k
$\eta$	—	Efficiency
$\eta_{Axledrive}$	—	Axle drive efficiency
$\eta_{CET}$	—	Efficiency of the contactless energy transmission system
$\eta_G$	—	Gear efficiency
$\eta_{iEESM}$	—	Efficiency of the iEESM
$\eta_{M,max}$	—	Maximum machine efficiency
$\eta_{OP}$	—	Efficiency at operation point
$\gamma$	rad	Viewing angle in the air-gap of the electrical machine

Symbol	Unit	Description
$\mu_0$	$V^s/A \cdot m$	Vacuum permeability
$\lambda_d$	Vs	d-Axis flux linkage
$\lambda'_e$	Vs	Referred excitation flux linkage
$\lambda_q$	Vs	q-Axis flux linkage
$\lambda$	Vs	Flux linkage
$\lambda_1$	Vs	Primary side flux linkage
$\lambda_{1\sigma}$	Vs	Primary side leakage flux linkage
$\lambda_2$	Vs	Secondary side flux linkage
$\lambda_m$	Vs	Main flux linkage
$\lambda_{\sigma 2}$	Vs	Secondary side leakage flux linkage
$\nu$	—	Count variable of a sums
$\nu_T$	—	Torque harmonic count
$\pi$	—	Mathematical constant
$\rho_{air}$	$kg/m^3$	Mass density of the air
$\sigma_{mech}$	MPa	Mechanical stress
$\sigma_{mech,peak}$	MPa	Mechanical stress in particular points
$\sigma$	$N/m^2$	Shear stress
$\tau_p$	mm	Pole width (air-gap center)
$\vartheta_{EWdg,R}$	$^{\circ}C$	Rotor end winding temperature
$\vartheta_{EWdg,S}$	$^{\circ}C$	Stator end winding temperature
$\vartheta$	$^{\circ}C$	Temperature
$\vartheta_{vent,in}$	$^{\circ}C$	Ventilation air inlet temperature
$\vartheta_{vent,out}$	$^{\circ}C$	Ventilation air outlet temperature
$\vartheta_{fl,in}$	$^{\circ}C$	Fluid inlet temperature
$\vartheta_{fl,out}$	$^{\circ}C$	Fluid outlet temperature
$\vartheta_{Wdg,R}$	$^{\circ}C$	Rotor winding temperature
$\vartheta_{Wdg,S}$	$^{\circ}C$	Stator winding temperature
$\omega$	$1/s$	Electrical angular frequency of the stator